Plant Stress 10 (2023) 100236

Contents lists available at ScienceDirect

Plant Stress

journal homepage: www.sciencedirect.com/journal/plant-stress

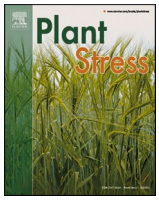

Comet assay as an early predictor tool to detect ozone enhanced sensitivity of vegetation in a free-air controlled long-term exposure

Roberta Meschini [a,*], Elena Paoletti [b], Yasutomo Hoshika [b], Zoi-Antigoni Sideri-Manoka [c], Ambra Dell'Orso [a], Giada Magni [d], Elena Kuzminsky [c]

[a] Department of Ecological and Biological Sciences (DEB), University of Tuscia, Via San Camillo de Lellis snc, 01100 Viterbo, Italy
[b] Institute of Research on Terrestrial Ecosystems (IRET), National Research Council of Italy (CNR), Via Madonna del Piano, I-50019 Sesto Fiorentino, Italy
[c] Department for Innovation in Biological, Agro-food and Forest Systems (DIBAF), University of Tuscia, Via San Camillo de Lellis snc, 01100 Viterbo, Italy
[d] Institute of Applied Physics (IFAC), National Research Council of Italy (CNR), Via Madonna del Piano, I-50019 Sesto Fiorentino, Italy

ARTICLE INFO

Keywords:
Ozone genotoxicity
O_3 Free air controlled exposure
Protoplast isolation
Comet assay
DNA damage
Ecophysiology

ABSTRACT

Although ozone (O_3) is a strong oxidant with serious impacts on plants, few studies have investigated the effects on DNA damage. Here we tested the Comet assay combined with the enzymatic isolation of leaf protoplasts. Two species differing in O_3 sensitivity were used, i.e. the moderately tolerant *Arbutus unedo* and the very sensitive *Populus maximowiczii* Henry × *berolinensis* (or Oxford clone), exposed to three O_3 levels (ambient [40.3 ppb], 1.5 times ambient O_3 concentration, twice ambient O_3 concentration) for one (*A. unedo*) or two (Oxford clone) growing seasons in an O_3 Free Air Controlled Exposure (FACE) facility. We found that O_3 has strong plant genotoxicity capacity and the negative effects increased with increasing exposure or stomatal uptake in both species. Interestingly, both ecophysiological and DNA damage were detected in the sensitive species, while no ecophysiological injury was observed in *A. unedo* although DNA was damaged before other symptoms occurred. Overall, DNA damage increased when the ecophysiological parameters decreased, confirming that DNA damage is a good proxy of the functional status of a plant. We conclude that the enzymatic isolation and Comet assay could be used as a predictor tool to reveal plant O_3 DNA damage even in moderately O_3 tolerant species, able to recover the abiotic stress.

1. Introduction

Ozone (O_3) in the troposphere is a major air pollutant with strong phytotoxic potential (Mills et al., 2018; Grulke and Heath, 2020). The O_3 concentration near the ground was no more than 10 ppb before the industrial revolution (Paoletti, 2007). The average annual concentration has increased up to 35–50 ppb in the northern hemisphere (Sicard et al., 2017). Predictions indicate that the exposure-based risk for vegetation in many areas of the Northern Hemisphere will be exceeded by a factor of at least 10 in 2100 (Sicard et al., 2017). In order to decrease O_3 pollution, European legislation has decided to regulate the emissions of O_3 precursors even because climate changes may further increase the O_3 levels (Young et al., 2013). In the Air Quality Guidelines of the World Health Organization the suggested level for human health was 60 ppb for 8-h mean concentration before 2005, and was later reduced to 50 ppb (WHO, 2021). About plant protection, AOT40 (Accumulated Ozone exposure over a Threshold of 40 ppb) is the legislative standard in Europe. A threshold of 5000 ppb h of AOT40 accumulated over the growing season has been suggested for forest trees corresponding to a 5 % growth reduction (CLRTAP, 2017). However, the O_3 risk assessment for forest trees is focused on stomatal O_3 flux because stomata are the principal interface for the O_3 entry into plants (Paoletti and Manning, 2007; Paoletti et al., 2022). The phytotoxic O_3 dose above an hourly stomatal O_3 flux threshold of 1 nmol m^{-2} s^{-1} (POD1) is currently recommended for explaining O_3 damage in forest trees (CLRTAP, 2017). In fact, previous studies demonstrated that POD1 was better correlated with an O_3-induced biomass reduction than AOT40 (e.g., Hoshika et al., 2018; Moura et al., 2021). CLRTAP (2017) reported a critical level of 4 mmol m^{-2} POD1 to protect the sensitive forest tree species, which corresponds to a 4 % biomass reduction.

Ozone can trigger necrosis in plants by causing visible injuries to the leaves, like pathogen infections and wounds do (Paoletti et al., 2019; Moura et al., 2022a); moreover, it causes faster leaf senescence (Hoshika et al., 2020a) and decreases photosynthesis (Hoshika et al., 2020b)

* Corresponding author.
E-mail address: meschini@unitus.it (R. Meschini).

https://doi.org/10.1016/j.stress.2023.100236
Received 28 July 2023; Received in revised form 14 September 2023; Accepted 24 September 2023
Available online 26 September 2023

thus inducing a general reduction of the plant growth (Hoshika et al., 2018; Paoletti et al., 2022). At present, O_3 uptake decreases gross primary production in 37.7 % of the northern-hemisphere forested area with a mean loss of 2.4 % year^{-1} (Anav et al., 2022). In addition, it causes stress-induced gene expression (Tseng and Lin, 2015; Marchica et al., 2019). Ozone enters inside the plant tissues from the stomata and induces oxidative stress enhancing the production of Reactive Oxygen Species (ROS) (Vainonen and Kangasjärvi, 2015), known to induce damage to cellular structures and molecules. At DNA level, the lesions induced by ROS form oxidative adducts cleavage of bases and DNA strand breakage (Aust and Eveleigh, 1999; Tuteja et al., 2001; Bjelland and Seeberg, 2003). However, plants have a complex network able to recognize the damaged DNA and perform efficient repair in order to maintain DNA functions (Yoshiyama et al., 2013). Ozone genotoxicity for microorganisms and animals is well known (Victorin, 1992), while for plants only few short-term studies are present in the literature and were carried out in closed or unreplicated open-top chambers (Rodrigues et al., 1996; de Souza Lima et al., 2009; Tai et al., 2010). As chamber effects are known to interfere with O_3 impacts on plants (Paoletti, 2007), long-term open-air exposure is recommended for experimentally validating the results of O_3 genotoxicity biomonitoring (Restivo et al., 2002; Piraino et al., 2006). The single cell gel electrophoresis (SCGE), also known as Comet assay, is a consolidated and validated genotoxicity test used to measure DNA damage (Langie et al., 2015). This assay is based on DNA strand break-induced relaxation of supercoiled loops, still attached to the nuclear matrix, which can migrate out of the nucleoid toward the anode under electric field, forming a tail. To the best of our knowledge, only Tai et al. (2010) and Restivo et al. (2002) employed this assay to measure O_3 genotoxicity in poplars and tobacco plants, respectively. However, both Restivo et al. (2002) and Tai et al. (2010) isolated nuclei by a mechanical approach, a procedure that could enhance the production of ROS. A new tool is the use of protoplast technology combined with SCGE assay for estimating DNA damage in plant leaf tissues under stress conditions (Kuzminsky et al., 2016; Choury et al., 2018). Besides, variation in cellular responses to DNA damage, in terms of repair activity, may greatly contribute to O_3 tolerance or sensitivity (Tai et al., 2010). Therefore, due to the gap of knowledge on O_3 genotoxicity on plant cells, the aim of the present work was to assess the DNA integrity through Comet assay in leaf protoplasts after exposure of plants of *Arbutus unedo* L. and *Populus maximowiczii* Henry × *berolinensis* Dippel, from now on referred as Oxford clone, to three realistic O_3 treatments that is ambient air, intermediate O_3 level and elevated O_3 level performed by a free-air controlled exposure (FACE) facility. The deciduous Oxford clone is known as very O_3 sensitive (Marzuoli et al., 2009; Zhang et al., 2018), while the Mediterranean evergreen *A. unedo* is considered as moderately sensitive to O_3 (Nali et al., 2004; Paoletti, 2006). A further goal was to investigate the relationships between the induced DNA damage and the responses of ecophysiological parameters. We postulate that O_3 has strong plant genotoxicity capacity and the negative effects increase with increasing exposure, and that Comet assay on enzyme-isolated protoplasts could be used as a predictor tool to reveal O_3 responses of vegetation.

2. Materials and methods

2.1. Plant material and free-air ozone exposure experimental design

The experiment took place in Sesto Fiorentino, Italy (43° 48′ 59″ N, 11° 12′ 01″ E, 55 m a.s.l.) in an open-air controlled exposure (FACE) facility. Ozone was produced by TOGC13X Mk2 compact ozone generator (Triogen Ltd., Scotland) with integral oxygen generator, diluted with ambient air in a mixing tank and injected into the FACE through 25 teflon tubes hanging down from a fixed grid above the plants (2 m height) in each of three plots per O_3 level. The O_3 concentration above plants (approx. 1.2 m height) was monitored continuously (Mod. 202, 2B Technologies, Boulder CO, USA), and the observed value was used as feedback to the valves to regulate the O_3 emission, using the proportional–integral–derivative algorithm (PID). More details on the O_3 FACE are described in Paoletti et al. (2017). There were three plots per each of three O_3 treatments ($n = 3$ plots), i.e.: ambient air (AA: 40.3 ppb as an hourly mean O_3 concentration during the experimental period in 2017), intermediate O_3 level ($O_3$1, 1.5 times ambient O_3 concentration) and elevated O_3 level ($O_3$2, twice ambient O_3 concentration).

In each plot there were 3 plants for *A. unedo* and 6 plants for Oxford clone. For both species the plant material was two years old. These three O_3 treatments were applied to *A. unedo* plants from 12th June to 15th October 2017, and to Oxford clone plants during two growing seasons (1st May to 1st October 2016, and 12th June to 15th October 2017). Two-year-old plants of *A. unedo* with uniform size (average height: 94.0 cm) were obtained from a local nursery on 4th May 2017 and transferred to the FACE on 17th May 2017 where they were transplanted in pots of 30 L and deprived of the terminal buds of the main axis to allow the emission of new soft leaves suitable for the Comet assay. One-year-old rooted cuttings of Oxford clone (average height: 15.4 cm) propagated in December 2015 were planted in plastic pots of 10 L in April 2016 and transferred to 20 L pots in April 2017 in order to avoid limitation of root growth. The soil was a 1:1:1 mixture of nursery soil:sand:peat. Every two or three days all plants were irrigated to avoid water stress, i.e., volumetric soil water content was nearly equal to field capacity (0.295 m^3 m^{-3}).

AOT40 for the two species was calculated according to CLRTAP (2017) i.e. as the sum of the hourly values over the threshold of 40 ppb over the O_3 exposure periods.

2.2. Analysis of DNA integrity

2.2.1. Protoplast isolation

For protoplast isolation, leaf tissue of ~0.045 g from young, fully expanded leaves (8th from the apex) gathered from three plants for every O_3 treatment, one for each plot, avoiding the main rib and using only the middle part. Leaf samples were taken, from 10.00 to 11.00 AM, on July 21th, August 30th and 31th and September 15th, 2017. It is worth noting that the leaves collected for protoplast isolation did not show any visible symptom of leaf injury (Fig. 1S).

Dim light conditions were used to obtain leaf protoplasts of both species. Leaves were put into the Cell and Protoplast Washing (CPW) solution added with a thin layer of Polyvinylpyrrolidone (PVP-40) powder, scratched with a sterile scalpel to partially remove epidermis and sliced in little pieces (Kuzminsky et al., 2016; Choury et al., 2018). Leaves strips (0.5 × 0.5 cm) were left inside the CPW solution for 10 min. Afterwards, strips were moved to a 35 mm Petri dish containing 2.5 ml of filtered (0.45 μm) enzyme solution composed by Macerozyme R-10 (1 %) and Cellulase Onozuka RS (2 %), freshly added with DTT (2 mM) to a solution at a pH 5.0 containing mannitol (0.6 M), KH_2PO_4 (1 mM), NH_4NO_3 (5 mM) and sodium citrate (5 mM). To inactivate DNAse and proteases and enhance enzyme solubility, the enzyme solution was pre-heated at 55 °C before using it. After Carbenicillin and Cefotaxime (0.5 % v/v) and PVP-40 powder (1 % w/v) were freshly added to the Petri dishes, samples were put in the dark in a vacuum condition for 30 min and then digestion was performed at 25 °C with gentle orbital shaking (50 rpm) for 4 h. Then, release of protoplast was monitored by an inverted microscope. Lastly, protoplast suspensions were filtered (CellTrics® 50 μm mesh) into an Eppendorf tube with 0.5 ml of CPW before centrifuging at 1000 × g for 5 min and the protoplast pellet was re-washed by re-suspension in 1 ml of CPW and centrifuged again. Protoplasts were analyzed by Comet assay for DNA integrity and by confocal microscopy to evaluate their morphology.

2.2.2. Single cell gel electrophoresis

In order to analyze DNA integrity, the standard alkaline (pH > 13) Single Cell Gel Electrophoresis (SCGE), or Comet assay, was performed as previously described (Meschini et al., 2015). Shortly, 10 μl of

protoplast suspension were mixed with 90 µl of 0.75 % low melting point agarose and placed on slides previously pre-coated with a layer of 1 % normal melting point agarose. Afterwards, slides were incubated in lysis solution (2.5 M NaCl, 10 mM Tris–HCl, 100 mM EDTA, pH 10, with 1 % Triton and 10 % DMSO freshly added) at 4 °C over-night and then horizontally placed into an electrophoresis unit. Electrophoresis was conducted for 20 min at 25 V and 300 mA at 4 °C preceded by a 15 min incubation in electrophoresis buffer to allow DNA unwinding in the same buffer (1 mM EDTA, 300 mM NaOH, pH>13. Lastly, slides were washed three times with the Neutralization Buffer (0.4 M Tris–HCl, pH= 7.5) and stained with 50 µl ethidium bromide (20 µg/ml). Nucleoids were examined at × 400 magnification with an automatic image analyzer (Comet Assay III, Perceptive Instruments, UK) connected to a fluorescence microscope (Axioskop 2, Zeiss).

For each O_3 treatment level 100 damaged/undamaged nucleoids randomly selected from two slides were examined at × 400 magnification with an automatic image analyzer (Comet Assay III, Perceptive Instruments, UK) connected to a fluorescence microscope (Axioskop 2, Zeiss). To evaluate the amount of DNA damage, computer-generated % DNA in the tail (Tail Intensity, TI) values were used.

2.3. Analysis of ecophysiological parameters

2.3.1. Biomass measurements

Before the start of the O_3 fumigation in 2017, ten *A. unedo* plants were harvested to examine the biomass at time zero. In addition, at the end of the experiment (15th October 2017), all *A. unedo* plants were harvested. For Oxford clone, similarly, the initial biomass was assessed for ten plants before the start of the O_3 fumigation in 2016. A half set of plants (3 plants per each plot per each O_3 treatment) were used to assess the biomass after the first-year O_3 fumigation (1st October 2016). The other half set of Oxford plants were harvested on 15th October 2017. Leaves and fine roots (diameter < 2 mm) were dried at 70 °C and other woody parts were dried at 103 °C to reach a constant weight. Dry mass of each organ (i.e., stem, branch, leaf and root) was determined by a balance (Mod. Bp110, Sartorius weighing technology, Germany). Annual biomass increments for *A. unedo* during the experiment in 2017 were evaluated by [(biomass at the end of experiment) - (biomass at the beginning of the experiment)] while this parameter for Oxford clone was calculated as [(biomass at the end of experiment) - (biomass at the end of the first-year fumigation)].

2.3.2. Leaf gas exchange

Leaf gas exchange was measured in fully expanded sun leaves (5th to 8th order from the shoot tip, 1 to 3 plants per each plot per each O_3 treatment per species) using a portable infra-red gas analyzer (CIRAS-2 PP Systems, Herts, UK) at controlled values of CO_2 concentration (Ca: 400 ppm), leaf temperature (25 °C) and of leaf-to-air vapor pressure deficit (VPD, 1.0–1.8 kPa) under light-saturated conditions (PPFD, Photosynthetic Photon Flux Density: 1500 µmol mol^{-1}). Measurements were carried out before (1 June 2017 for *A. unedo* and 29 May 2017 for Oxford clone) and after O_3 exposure (17th July, 6th and 29th-30th September 2017 for *A. unedo*,14th July, and 14th-15th September 2017 for Oxford clone) to determine a seasonal variation of the light-saturated net photosynthetic rate (Asat). In addition, in September (29th-30th September 2017 for *A. unedo*, and 14th-15th September 2017 for Oxford clone), to assess the photosynthetic capacity, we also measured the response curve of net photosynthesis (A) to C_i, i.e., the A/C_i curve, with nine steps of CO_2 concentration [C_a: 400, 200, 100, 50, 400, 700, 1100, 1500, 2000 ppm] in both species under the same conditions of PPFD, temperature and humidity. We determined A at 400 ppm (Asat) and 2000ppm (*A2000*), stomatal conductance (gs), the maximum carboxylation rate (V_{cmax}) and the maximum electron transport rate for Ribulose-1,5-bisphosphate (RuBP) regeneration (J_{max}) by the curve fitting method in accordance with Long and Bernacchi (2003). The values of Michaelis constants for CO_2 (K_c) and O_2 (K_o) and the CO_2 compensation point in the absence of dark respiration (Γ^*) for the analysis of the A/C_i curve were derived according to Bernacchi et al. (2001). All gas exchange measurements were made on days with clear sky between 8:00 and 12:00.

2.3.3. Leaf traits

After the measurement of leaf gas exchange in September 2017, the measured leaves in both species were collected in order to determine the leaf mass per unit area (LMA). The projected leaf area was determined by a portable leaf area meter (Area Meter AM300, ADC Bioscientific Ltd, UK). The collected leaves were dried in an oven at 70 °C for one week and then weighed. The LMA was calculated as the ratio of dry mass to the area of the leaves.

2.3.4. Visible foliar injury

Ozone-induced visible foliar injuries were assessed according to the protocol established by ICP-Forests (Schaub et al., 2016). Two well-trained observers evaluated the onset of foliar symptoms every two weeks during the experiment in 2017. The symptoms were also confirmed by photo-references (Innes et al., 2001; Hoshika et al., 2013; Moura et al., 2022b).

2.4. Estimation of stomatal ozone uptake (POD1)

The phytotoxic O_3 dose above an hourly stomatal O_3 flux threshold of 1 nmol m^{-2} s^{-1} (POD1) in both species during the experiment was determined according to the standard method proposed by CLRTAP (2017). POD1 can be estimated by the DO3SE model considering species specific g_s responses to various meteorological factors (CLRTAP, 2017). Here, we used the simplified formula for the estimation of stomatal conductance for O_3 (g_{sO3}) in the DO3SE model (Hoshika et al., 2020c):

$$g_{sO3} = g_{max} \cdot f_{light} \cdot max\{f_{min,} \ (f_{temp} \cdot f_{VPD}) \ \} \quad (1)$$

where g_{max} is the maximum stomatal conductance (mmol O_3 m^{-2} projected leaf area (PLA) s^{-1}), f_{min} is the minimum conductance, and f_{light}, f_{temp} and f_{VPD} denote the effects of PPFD, air temperature and vapor pressure deficit on stomatal conductance, respectively. The parameterization of the DO3SE model for Oxford clone and *A. unedo* was already achieved in our previous works (Hoshika et al., 2018b; Moura et al., 2022b). The detailed parameters are shown in the Supplementary file (Table S3).

2.5. Data analysis

All data were tested for normal distribution by Kolmogorov-Smirnov D-test, with the exception of TI data analyzed by Shapiro-Wilk W test, and homogeneity of variance (Levene's test). Since data were normally distributed, we applied a three-way analysis of variance (ANOVA) to examine the effects of O_3, species and measured month on TI values. In addition, a two-way ANOVA was also used to test the effect of O_3 and species on LMA and biomass and photosynthetic parameters. A quadratic regression was applied to examine the relationships between A_{sat} and POD1 for both species. These statistical analyses were performed by R software (R 3.5.1, R Core Team). To compare long-term impacts of O_3 exposure on DNA damage, linear regressions between POD1 or AOT40 values at the sampling date and TI values were carried out. Pearson's coefficient was calculated to evaluate the correlation between TI and AOT40 or POD1 using Past3 software. Spearman correlation was tested among TI, biomass growth and gas exchange parameters.

3. Results

3.1. Ozone indices

AOT40 and POD1 values during the experimental period are given in Table 1. AOT40 values increased with increasing O_3 exposure levels (year 2016: +190 % in $O_3$1, +399 % in $O_3$2, year 2017: +92 % in $O_3$1, +177 % in $O_3$2). POD1 values depended on the species. *A. unedo* had a lower POD1 value than Oxford clone regardless of the O_3 treatment.

3.2. Ozone effect on DNA integrity

TI values usually increased from July to August, while in September they were stable or even lower for both the species, with statistical significance only for Oxford clone (Table 2).

In *A. unedo*, after about 1- and 2-months of exposure to O_3, the mean TI values significantly increased in both $O_3$1 ($p<0.01$; $p<0.05$) and $O_3$2 ($p<0.001$) as compared to AA. In addition, in August, plants under $O_3$2 treatment showed significantly ($p<0.05$) higher mean TI values than in July. In September, the mean TI values significantly ($p<0.001$) increased only in $O_3$2 with respect to AA.

In Oxford clone, after about 1- and 2-months of exposure to O_3, the mean TI values significantly increased in both $O_3$1 ($p<0.001$) and $O_3$2 ($p<0.001$) as compared to AA. Conversely to *A. unedo*, in August plants under $O_3$1 treatment showed significantly ($p<0.05$) higher mean TI values than in July. In September, although the mean TI values increased significantly in both $O_3$1 ($p<0.05$) and $O_3$2 ($p<0.01$) in comparison with AA, the level of the mean TI in both the O_3 exposed plants were lower than in July and August.

Finally, comparing the two species in August and September, TI values in AA in *A. unedo* were significantly ($p<0.05$) higher than the corresponding Oxford clone samples. Additionally, in September the exposure to $O_3$2 determined a significant ($p<0.001$) increase of TI values in *A. unedo* as compared to the same O_3 treatment in Oxford clone.

During the experiment, both AOT40 and POD1 positively correlated with TI values reaching high values ranging from 0.85 to 1 after about 1-, 2- and 3-months of exposure (Fig. 1A, B). Nevertheless, in Oxford clone at each sampling date the relationships between TI and both AOT40 and POD1 showed a similar trend but with a decrease in the slope along the experiment, due to the lower TI values detected in September compared to the previous months. Conversely, in *A. unedo* the relationships between TI and AOT40 or POD1 are different at each sampling date with a higher steepness of the line in the latter one (Fig. 1A, B).

3.3. Ozone effect on ecophysiological parameters

3.3.1. Biomass growth

Elevated O_3 exposure did not significantly affect plant biomass development in *A. unedo* (Fig. 2, Table S1). On the other hand, annual biomass increment was significantly reduced by O_3 for Oxford clone during the experiment in 2017 (–18 % at $O_3$1, –32 % at $O_3$2). The negative effect was confirmed regardless of the different organs as it was found in leaf (year 2016: –37 % at $O_3$1, –54 % at $O_3$2, year 2017: –57 % at $O_3$1, –85 % at $O_3$2), coarse root (year 2016: –34 % at $O_3$1, –39 % at $O_3$2, year 2017: –20 % at $O_3$1, –32 % at $O_3$2) and fine root biomass (year 2017: –3 % at $O_3$1, –22 % at $O_3$2) in Oxford clone (Table S2).

Table 1
AOT40 (accumulated exposure over a threshold of 40 ppb) and POD1 (phytotoxic ozone dose above an hourly stomatal O_3 flux threshold of 1 nmol m^{-2} s^{-1}) for *A. unedo* and Oxford clone of poplar during the experimental period in 2016 (1st May to 1st October) and 2017 (12th June to 15th October). Three O_3 levels (ambient air [AA], 1.5 times ambient O_3 concentration [$O_3$1], and twice ambient O_3 concentration [$O_3$2]) were applied.

Year 2016			
	AA	$O_3$1	$O_3$2
AOT40 (ppm·h)	14.4	41.8	71.8
POD1 (mmol m^{-2})			
Oxford clone	30.9	45.4	63.4
Year 2017			
	AA	$O_3$1	$O_3$2
AOT40 (ppm·h)	21.8	41.8	60.3
POD1 (mmol m^{-2})			
A. unedo	3.1	5.0	6.9
Oxford clone	28.1	35.8	42.9

Table 2
Mean Tail Intensity values (± S.E., $n = 3$ plants) in *A. unedo* and Oxford clone treated with three levels of O_3 (ambient air [AA], 1.5 times ambient O_3 concentration [$O_3$1], and twice ambient O_3 concentration [$O_3$2]) during the experiment in 2017.

	Source material	Tail Intensity% July 21st	August 31th	September 15th
Arbutus unedo	***AA***	1.56±0.41e	7.47 ±0.73d	9.16±1.1cd
	$O_3$1	8.62±2.01cd	13.07 ±1.98bc	10.19±1.56cd
	$O_3$2	12.85 ±2.02bc	20.47 ±1.99a	15.06±1.08ab
	Source material	**Tail Intensity%** July 21st	August 30st	September 15th
Oxford clone	AA	2.06±0.3d	5.47 ±0.48c	6.16±0.43c
	$O_3$1	9.19±1.07b	13.99 ±1.08a	8.31±0.7b
	$O_3$2	13.36 ±2.46ab	16.46 ±1.38a	9.29±0.87b
Anova	Sp. ns O_3 *** M ***		Sp.xO_3 ns Sp.xM * O_3xM * Sp.xO_3xM ns	

Different letters show significant differences among treatments in each species ($p < 0.05$, Anova). Sp.: Species; ns: not significant; M: month.

3.3.2. Leaf traits and visible foliar injuries

No difference in LMA was recorded among O_3 treatments regardless of species (data not shown). Mean values of LMA were 131.3 g m^{-2} in *A. unedo* and 87.8 g m^{-2} in Oxford clone.

On leaves of Oxford clone, first visible symptoms were observed on 20th July 2017 under $O_3$2 treatments. Brown spots were found in interveinal areas of upper leaf surface (Fig. 5D). On the other hand, reddish lesions emerged for A. unedo leaves exposed to $O_3$2 on 18th September 2017 (Fig. 5E).

3.3.3. Leaf gas exchange parameters

Leaf gas exchange parameters are shown in Table 3, Table S4 and Fig. 3. Both A_{sat} and g_s were higher in Oxford clone than in *A. unedo*. This can be also confirmed by the fact that g_{max} was lower in *A. unedo* (95 mmol O_3 m^{-2} PLA s^{-1}) than in Oxford clone (345 mmol O_3 m^{-2} PLA s^{-1}) (Table S3). The relationship between Asat and POD1 for *A. unedo* showed a quadratic curve with a slight increase in the photosynthetic rate during summer and then a decreased photosynthesis was observed especially in the highest O_3 treatment ($O_3$2) (Fig. 3; Table S4). On the other hand, Asat for Oxford clone was decreasing with increasing POD1 especially when POD1 was higher than 20 mmol m^{-2} (Fig. 3). There was no effect of O_3 on photosynthetic parameters for both species in July (Table S4). However, twice ambient O_3 concentrations significantly decreased A_{sat} in September in both species (Table 3, Oxford clone:–53 % at $O_3$2; *A. unedo*: –30 % at $O_3$2). Accordingly, stomatal conductance was significantly reduced by twice ambient O_3 exposure in *A. unedo* (–45 % at O32). However, such a significant reduction was not found in Oxford clone according to the Tukey test. In addition, O_3-exposed Oxford clone leaves had significantly lower V_{cmax}, J_{max} and A_{2000} in $O_3$2 than in AA whereas no significant difference in those parameters was

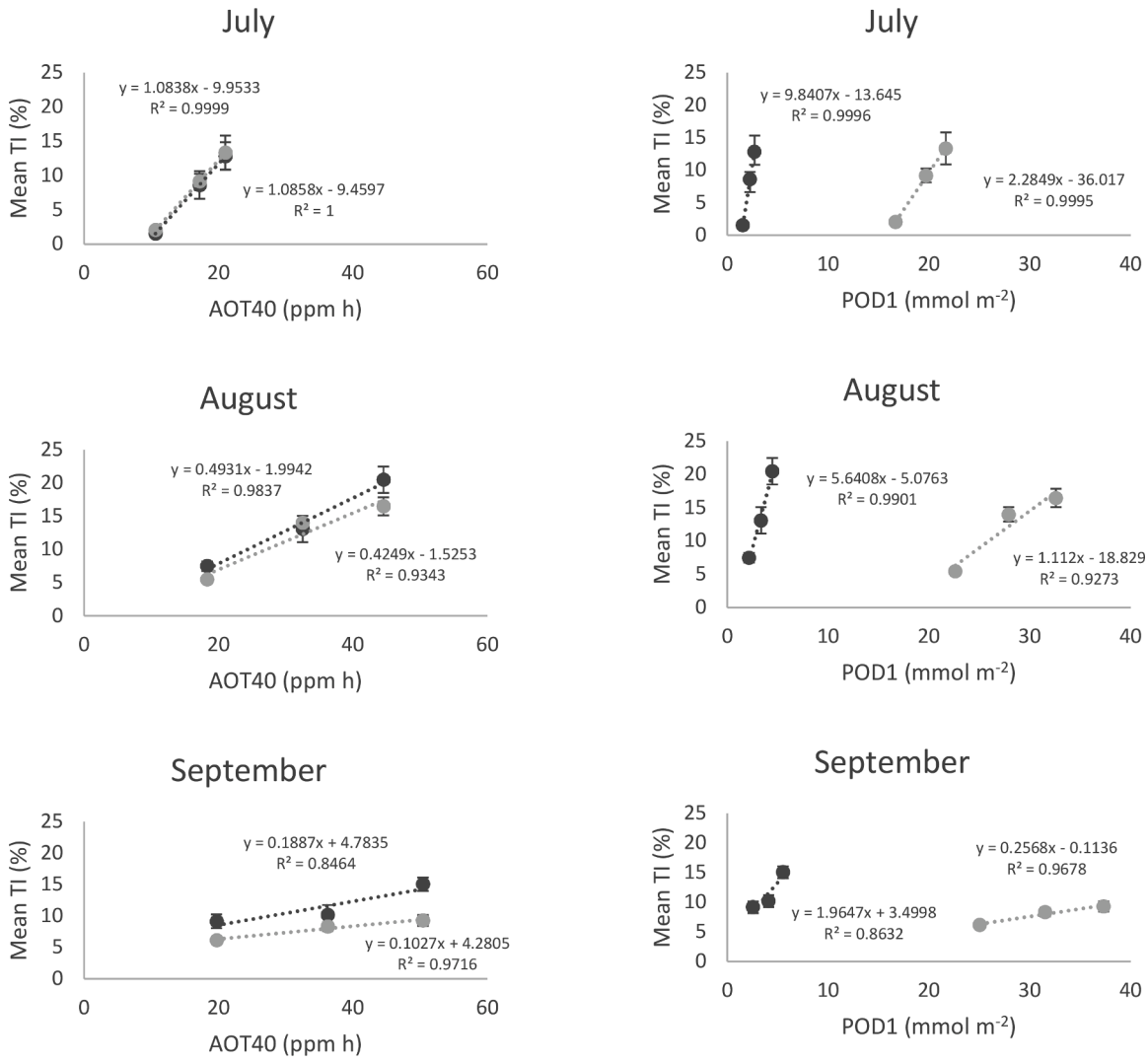

Fig. 1. Tail Intensity and O_3 exposure or stomatal uptake relationship. Linear relationships between AOT40 (A) or POD1 (B) and mean Tail Intensity values in both species (Black circle: *A. unedo*; grey circle: Oxford clone) in July, August and September.

found among the O_3 treatments in *A. unedo* (Table 3).

3.4. Correlation of DNA damage with biomass and ecophysiological responses

When TI increased, the gas exchange parameters decreased although the response was not significant for Vcmax (Fig. 4). No correlation between TI and annual biomass growth was observed. Annual biomass growth varied significantly only with Vcmax.

4. Discussion

Owing to a gap of knowledge, O_3 genotoxicity on plant cells is still under debate (Singh, 2022). The present study assessed DNA integrity after exposure of plants of two species differing in O_3 sensitivity, i.e. the moderately sensitive *A. unedo* and the highly sensitive Oxford clone, to three O_3 treatments under open-air conditions that is ambient air, intermediate O_3 level (1.5 times ambient) and elevated O_3 level (twice ambient). This innovative FACE system gave us the opportunity to better simulate the actual environmental conditions (Paoletti et al., 2017). A FACE facility represents a chronic O_3 exposure in contrast to an acute one, although, in $O_3$2 only, during August, 14 days out of 31 (data not shown) were characterized by O_3 exposure equal or higher than 150 ppb h 8 h (8:00–16:00), that is considered acute exposure condition (Turcsanyi et al., 2000).

DNA integrity was assessed using leaf protoplasts combined with the Comet assay. As far as we are concerned, this is the first time that leaf protoplasts were employed for the implementation of the Comet assay in order to measure DNA damage in an O_3 FACE facility. On the other hand, *A. unedo* (Choury et al., 2018) and *Populus alba* (Kuzminsky et al., 2016) were already tested for the Comet assay through mesophyll protoplasts, resulting in suitable plant material. Another similar study in which the Comet assay was used to measure O_3-induced DNA damage in the Aspen FACE project (Karnosky et al., 2001) was the one by Tai et al. (2010) in poplar, where nuclei isolation from frozen leaves were obtained with a scalpel blade which could lead to the enhancement of ROS (Ackah et al., 2022). Conversely, the enzymatic method employed for the present study allowed the isolation of healthy protoplasts in a very short time (4 h), ensuring a reduced oxidative stress, as shown by a very low mean TI values in ambient O_3 treatment in the first sampling (July 21th), due to a high rate of undamaged protoplasts (Table 2). In addition, besides mesophyll protoplasts, the procedure allowed also the isolation of guard cells protoplasts (Fig. 5A-C). Considering that guard cells constitute the first defensive barrier, it would be interesting to develop protocols for their separation from those of the mesophyll since they could reveal a greater sensitivity to the induction of DNA damage, in particular following O_3 exposure.

During the experiment (from June 12th to October 15th 2017) the

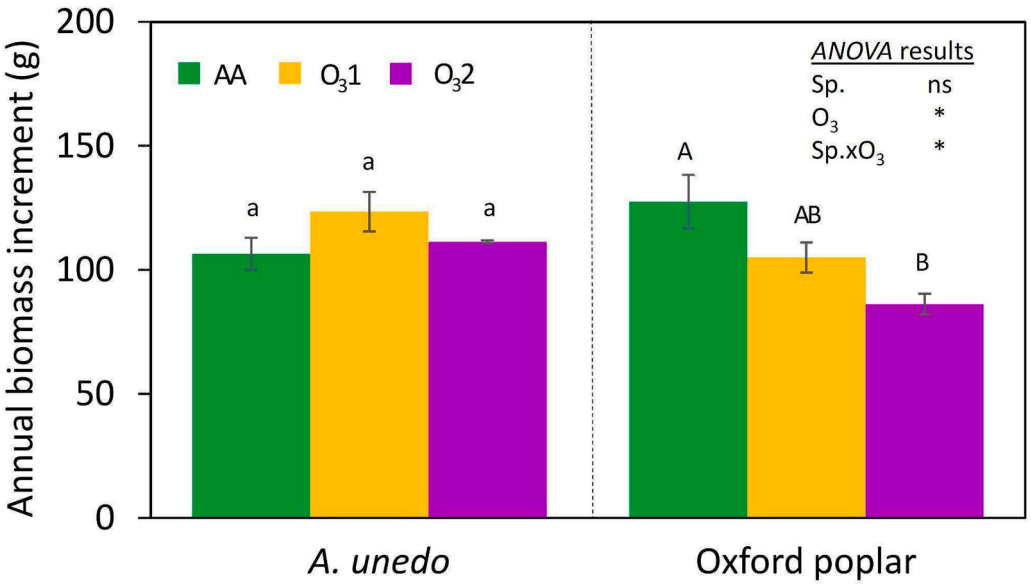

Fig. 2. Effect of O_3 exposure on annual biomass. Annual biomass increment during the experiment in 2017 for *A. unedo* and Oxford clone grown under three O_3 concentrations (ambient air [AA], 1.5 times ambient O_3 concentration [$O_3$1], and twice ambient O_3 concentration [$O_3$2]). The bars represent mean±*S.*E. ($n = 3$ plots). A two-way ANOVA was applied to test the effects of species (Sp.), O_3 and their interactions, *, $p < 0.05$; ns, not significant. Different letters show significant differences among treatments in each species ($p < 0.05$, Tukey test).

Table 3
Photosynthetic parameters derived from A/C_i curves in leaves of Oxford clone and *A. unedo* in September 2017 under three O_3 concentrations (ambient air [AA], 1.5 times ambient O_3 concentration [$O_3$1], and twice ambient O_3 concentration [$O_3$2]). A_{sat}: light-saturated net photosynthetic rate at 400 ppm CO_2, g_s: stomatal conductance, V_{cmax}: maximum rate of carboxylation, J_{max}: maximum rate of electron transport, A_{2000}: net photosynthetic rate at 2000ppm CO_2. Each value is the mean (±*S.*E.) of three replicated plots.

	A_{sat} (μmol m^{-2} s^{-1})		g_s (mol m^{-2} s^{-1})		V_{cmax} (μmol m^{-2} s^{-1})	
Arbutus unedo						
AA	10.3 ± 0.8	a	0.13 ± 0.01	A	60.2 ± 5.8	A
$O_3$1	10.0 ± 0.9	ab	0.10 ± 0.01	A	58.6 ± 4.9	A
$O_3$2	7.2 ± 0.1	b	0.07 ± 0.00	B	46.5 ± 3.8	A
Oxford clone						
AA	16.9 ± 0.8	A	0.44 ± 0.04	A	59.1 ± 2.8	A
$O_3$1	11.2 ± 0.6	B	0.42 ± 0.01	A	41.1 ± 2.8	B
$O_3$2	7.9 ± 1.6	B	0.38 ± 0.03	A	29.6 ± 4.9	B
ANOVA results						
Sp.	**		***		**	
O_3	***		*		**	
Sp. × O_3	*		Ns		Ns	
(Continue)						
	J_{max} (μmol m^{-2} s^{-1})		A_{2000} (μmol m^{-2} s^{-1})			
Arbutus unedo						
AA	95.3 ± 5.1	A	17.7 ± 0.8	a		
$O_3$1	91.7 ± 3.6	A	17.5 ± 0.4	a		
$O_3$2	92.0 ± 2.9	A	18.5 ± 0.8	a		
AA	117.0 ± 5.9	A	23.0 ± 1.5	A		
$O_3$1	96.7 ± 8.2	AB	19.8 ± 1.3	A		
$O_3$2	70.6 ± 5.6	B	14.2 ± 1.0	B		
ANOVA results						
Sp.	Ns		Ns			
O_3	**		**			
Sp. × O_3	**		**			

A two-way ANOVA was applied to test the effects of species (Sp.), O_3 and their interactions, ***, $p < 0.001$; **, $p < 0.01$; *, $p < 0.05$; ns, not significant. Different letters show significant differences among treatments in each species ($p < 0.05$, Tukey test).

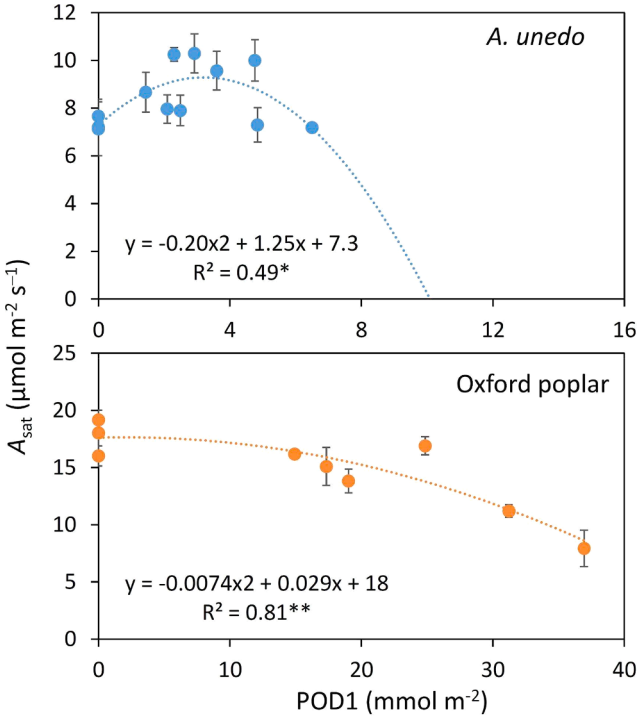

Fig. 3. Net photosynthetic rate and O_3 stomatal uptake relationship. Relationship between light-saturated net photosynthetic rate (A_{sat}) and phytotoxic O_3 dose (POD1) of *A. unedo* and Oxford clone grown under three O_3 concentrations (ambient air [AA], 1.5 times ambient O_3 concentration [$O_3$1], and twice ambient O_3 concentration [$O_3$2]). The data points represent mean±*S.*E. ($n = 3$ plots). A quadratic regression was applied: **, $p < 0.01$; *, $p < 0.05$. The detailed information of data can be found in Table S4.

meteorological conditions were particularly hot and dry (Paoletti et al., 2019), resulting in high AOT40 values (Table 1). The peak of temperature (higher than 40 °C) was from the end of July to the beginning of August, soon after the first sampling for the Comet assay and ecophysiological measurements. The total precipitation was 191 mm. However, the plants were sufficiently irrigated, to avoid water stress.

The results of Comet assay revealed an increasing DNA damage with the enhancement of both AOT40 and POD1, as confirmed by high

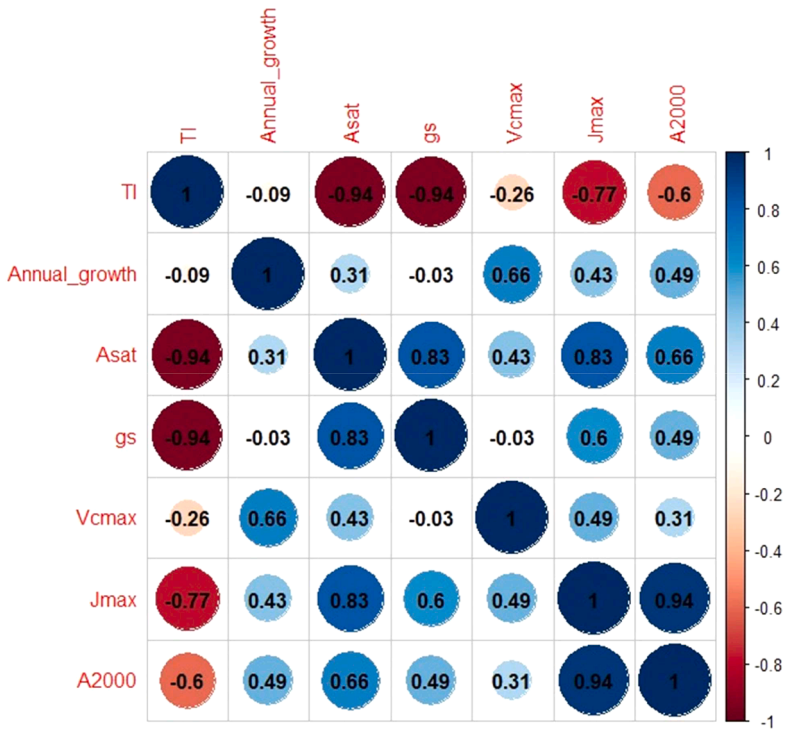

Fig. 4. Spearman coefficients in the correlation of DNA damage (TI) with annual biomass growth and ecophysiological parameters (for the acronym meaning, see Table 3).

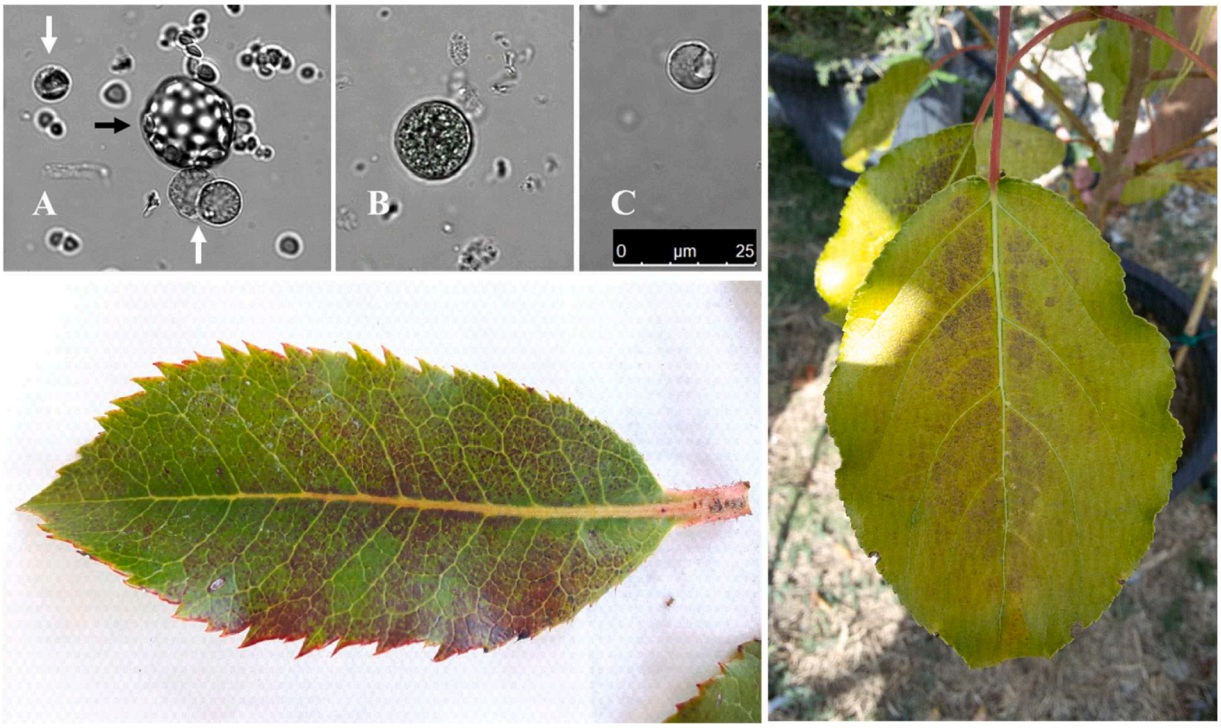

Fig. 5. Isolated protoplasts and foliar injury. Confocal images protoplasts isolated by enzymatic method from mesophyll cells and stomatal cell guards (A-C). Oxford poplar (A), black arrow points at a mesophyll protoplast and white arrows point at guard cell protoplasts. *A. unedo,* mesophyll protoplast (B) and guard cell protoplast (C). Example of foliar injury observed in the bottom part of the plants in Oxford poplar in the twice ambient O_3 concentration [$O_3$2] treatment (D) at the end of July. Example of foliar injury in *A. unedo* in the twice ambient O_3 concentration [$O_3$2] treatment (E) observed in late September.

correlation coefficients (Fig. 1). These results confirm that Comet assay is a rapid and sensitive technique to reveal early DNA damage in isolated protoplasts before the onset of visible leaf injury, in accordance with Dell'Orso et al. (2021); moreover, Comet assay is a very sensitive method to quantify single and double strand breaks detectable at the moment of sample collection.

Taking advantage of this technique, for the first time in the present study, correlations between mean TI and AOT40 or POD1 were

described for both species. Regarding Oxford clone, the similar decrease of the slopes observed in the two correlations along the experiment can be explained with the high g_s values of this species that may favor O_3 uptake and lead to cell death in the most exposed portion of the leaf. It is worth noting that the apoptotic process involves DNA fragmentation to the size of oligonucleotides which is not detectable by Comet assay; moreover, conventional computerised image analysis systems have difficulties in correctly evaluate these type of comets (Azquesta and Collins, 2013). In this context, the reduction of TI values observed in September could be attributed to heavily damaged cells. Concerning *A. unedo*, the difference in the slopes between the two correlations can be ascribed to a controlled stomatal O_3 uptake of the strawberry tree, allowing an efficient repair of the induced DNA damage at all levels of exposure.

Besides, regarding correlations between mean TI and AOT40, the two species almost overlapped (Fig. 1A). Thus, the different response to O_3 treatment of the two species cannot be highlighted using the AOT40 index. Conversely, considering correlations between mean TI and POD1 the two species differed in their response to O_3 all along the experiment and at all levels of exposure (Fig. 1B). Indeed, even though AOT40 and POD1 are both O_3 indexes, the latter is a better one since it reflects the actual leaf adsorbed O_3, while AOT40 estimates only O_3 concentration in the air (Sacchelli et al., 2021). These data emphasised the influence of the different sensitivity of the two species in terms of the relationship between DNA damage and the level of O_3 exposure.

Moreover, in late July the onset of a visible foliar injury in Oxford clone was observed (Fig. 5D). It is worth noting that protoplast isolation from injured leaf was well-nigh impossible, probably due to leaf aging associated with hardened tissues as previously reported by Choury et al. (2018). Concerning *A. unedo*, the first visible injury was observed in late September with only few leaves presenting some reddish symptoms (Fig. 5E), even though the threshold of 31.5 ppm h AOT40 reported by Nali et al. (2004) as necessary to reveal a macroscopic leaf damage in this species over a period of 3 month was exceeded in both $O_3$1 and $O_3$2 treatments.

These apparent contradictory results could be explained with a chronic O_3 exposure in open air in the present study in contrast with an acute O_3 exposure in the experiment conducted by Nali et al. (2004) in closed chambers.

Then, in September, in Oxford clone both $O_3$1 and $O_3$2 induced lower TI values as compared to the previous months (Table 2). This unexpected behavior could be related to the inability to activate repair strategies when O_3 sensitive plants, such as Oxford clone, are exposed to the most stressful conditions, as observed in the same FACE facility at the end of the growing season (Podda et al., 2019). The lack of repair strategy activation could lead to cell death and, hence, to a reduction of DNA damage detected by Comet assay (Bankoglu et al., 2021). For what concern *A. unedo*, the higher DNA damage than in Oxford clone could suggest the onset of repair events leading to transient single strand breaks as well as DNA lesions both detected by standard Comet assay, in agreement with Tai et al. (2010). Indeed, this approach can be performed to reveal single-strand break, double-strand break, oxidative DNA damage, and single-strand break related to incomplete excision repair sites caused by both physical and chemical agents (Collins, 2014).

A further goal of the present study was to find a relationship between the induced DNA damage and the responses of ecophysiological parameters. DNA damage increased when the ecophysiological parameters were negatively affected (Fig. 4). This result is novel for O_3 and confirms that DNA damage is a good proxy of the functional status of a plant.

During the experiment, both A_{sat} and g_s values resulted significantly higher in Oxford clone than in *A. unedo*, according to the autecology of these species. Moreover, in July no significant effects of O_3 treatments in both species were observed (Table S4), while Comet assay data already revealed a significant increase of DNA damage in both Oxford clone and *A. unedo*. Also, Dell'Orso et al. (2021) found that Comet assay can be suggested as a predictive test to detect DNA damage before other symptoms occur. However, the two species showed an overlapping behavior for ecophysiological parameters as well as for Comet assay results, suggesting that after about 1 month of exposure to O_3 they did not diverge in their response to O_3 treatments. In September, *A. unedo* plants showed a significant decrease in A_{sat} and g_s under $O_3$2 treatments, although the V_{cmax} and J_{max} in leaves of *A. unedo* were not significantly affected by O_3 treatments (Table 3). This result indicates that the O_3-induced reduction of photosynthetic rate in *A. unedo* was mainly due to stomatal diffusive limitation to CO_2 transfer. Conversely, Oxford clone plants showed a significant A_{sat} decrease in both $O_3$1 and $O_3$2; in addition, this was accompanied by a significant reduction of V_{cmax} and J_{max}, suggesting a damage to the biochemical component of photosynthetic systems. In line with this statement, it has been previously demonstrated that O_3 exposure leads to reduced Rubisco activity (Watanabe et al., 2014a, b, Bagard et al., 2015) associated with a decrease in the maximum rate of carboxylation (Hoshika et al., 2022). The divergent species-specific response to O_3 exposure, revealed at the end of the experiment, could be ascribed to an efficient stomatal restriction of O_3 uptake in *A. unedo* not detected in Oxford clone, as further confirmed by a higher POD1 value in Oxford clone than in *A. unedo*.

The different sensitivity between the two species was also accounted by a significant reduction of total biomass only in Oxford clone (Fig. 2; Tab. S2), while in *A. unedo* this parameter was not influenced by O_3 treatments (Fig. 2; Tab. S1). In addition, in the sensitive species, leaves were the most affected tissues with an 85 % reduction in biomass. Moreover, previous data reported a higher reduced glutathione (GSH) content mostly in a resistant Euromerican poplar genotype after O_3 treatment compared to a sensitive genotype (Dumont et al., 2014) while Nali et al. (2004) described a high enhancement of the same antioxidant enzyme in *A. unedo* in response to O_3 exposure. Thus, in *A. unedo* more defense mechanisms could be responsible for the higher tolerance to O_3 exposure such as a reduced POD1 value, functioning as an avoidance strategy and a more efficient antioxidant enzymatic system (Nali et al., 2004). Thus, the combination of ecophysiological approaches with molecular analysis of DNA integrity allows a better understanding of the state of the plant in relation to the induced stress as well as the assessment of its sensitivity.

5. Conclusion

In conclusion, in sensitive species such as Oxford clone, at an environmental exposure level that exceeds the threshold both in terms of AOT40 and POD1, both ecophysiological and DNA damages were detected. Conversely, at the same exposure levels, in moderately tolerant species like *A. unedo* no ecophysiological injury is observed but DNA is damaged in agreement with the early Comet lesions occurring before any other symptoms and associated with a progressive increase in sensitivity in terms of DNA damage. Therefore, the overall results confirm the use of Comet assay associated with enzyme-isolated protoplasts as an efficient predictive test to identify the DNA damage induced by O_3 (Dell'Orso et al., 2021). In addition, to the best of our knowledge, the study demonstrates for the first time the increased O_3 sensitivity revealed by Comet assay in a moderately tolerant species. Thus, this approach could be recommended also to predict changes in species responsiveness in relation to continued exposure to elevated O_3 levels such as those foreseen by future scenarios.

Funding

This work was supported by:
MIUR-PRIN (Grant No 20109E8F95);
PNRR for Mission 4 (Component 2, Notice 3264/2021, IR0000032) - ITINERIS - Italian Integrated Environmental Research Infrastructure System CUP B53C22002150006, and National Recovery; @CNR project 4ClimAir (SAC.AD002.173.019).

Declaration of Competing Interest

The authors declare that they have no known competing financial interests or personal relationships that could have appeared to influence the work reported in this paper.

Data availability

Data will be made available on request.

Acknowledgments

We are grateful to Alessandro Materassi, Elisa Carrari and Moreno Lazzara for technical support during plant rising and treatments.

Supplementary materials

Supplementary material associated with this article can be found, in the online version, at doi:10.1016/j.stress.2023.100236.

References

Ackah, S., Bi, Y., Xue, S., Yakubu, S., Han, Y., Zong, Y., Atuna, R.A., Prusky, D., 2022. Post-harvest chitosan treatment suppresses oxidative stress by regulating reactive oxygen species metabolism in wounded apples. Front. Plant Sci. 13, 959762 https://doi.org/10.3389/fpls.2022.959762.

Anav, A., De Marco, A., Emberson, L., Feng, Z., Lombardozzi, D., Sicard, P., Verbeke, T., Viovy, N., Vitale, M., Paoletti, E., 2022. Legislative and functional aspects of different metrics used for ozone risk assessment to forests. Environ. Pollut. 295, 118690 https://doi.org/10.1016/j.envpol.2021.118690.

Aust, A.E., Eveleigh, J.F., 1999. Mechanisms of DNA oxidation. Proc. Soc. Exp. Biol. Med. 222 (3), 246–252. https://doi.org/10.1046/j.1525-1373.1999.d01-141.x.

Azqueta, A., Collins, A.R., 2013. The essential comet assay: a comprehensive guide to measuring DNA damage and repair. Arch. Toxicol. 87, 949–968. https://doi.org/10.1007/s00204-013-1070-0.

Bagard, M., Jolivet, Y., Hasenfratz-Sauder, M.P., Gérard, J., Dizengremel, P., Le Thiec, D., 2015. Ozone exposure and flux-based response functions for photosynthetic traits in wheat, maize and poplar. Environ. Pollut. 206, 411–420. https://doi.org/10.1016/j.envpol.2015.07.046.

Bankoglu, E.E., Schuele, C., Stopper, H., 2021. Cell survival after DNA damage in the comet assay. Arch. Toxicol. 95, 3803–3813. https://doi.org/10.1007/s00204-021-03164-3.

Bjelland, S., Seeberg, E., 2003. Mutagenicity, toxicity and repair of DNA base damage induced by oxidation. Mutat. Res. - Fund. Mol. M. 531 (1–2), 37–80. https://doi.org/10.1016/j.mrfmmm.2003.07.002.

Bernacchi, C.J., Singsaas, E.L., Pimentel, C., Portis, Jr.A.R., Long, S.P., 2001. Improved temperature response functions for models of Rubisco-limited photosynthesis. Plant Cell Environ 24 (2), 253–259. https://doi.org/10.1046/j.1365-3040.2001.00668.x.

Choury, Z., Meschini, R., Dell'Orso, A., Fardusi, M.J., Mugnozza, G.S., Kuzminsky, E., 2018. Optimized conditions for the isolation of mesophyll protoplasts along the growing season from *Arbutus unedo* and their use in single cell gel electrophoresis. Plant Cell Tiss. Organ Cult. 132 (3), 535–543. https://doi.org/10.1007/s11240-017-1349-6.

CLRTAP, 2017. Mapping Critical Levels For Vegetation, Chapter III of Manual On Methodologies and Criteria For Modelling and Mapping Critical Loads and Levels and Air Pollution effects, Risks and Trends. UNECE Convention on Long-range Transboundary Air Pollution. http://icpvegetation.ceh.ac.uk/.

Collins, A.R., 2014. Measuring oxidative damage to DNA and its repair with the comet assay. Biochim. Biophys. Acta 1840 (2), 794–800. https://doi.org/10.1016/j.bbagen.2013.04.022.

Dell'Orso, A., Kuzminsky, E., Bermejo-Bermejo, V., Ruiz-Checa, R., Amo, R.A.D., Meschini, R., 2021. DNA integrity and ecophysiological responses of Spanish populations of *Ulmus glabra* to increasing ozone levels. ecotoxicol. 30 (6), 1098–1107. https://doi.org/10.1007/s10646-021-02436-z.

de Souza Lima, E., de Souza, S.R., Domingos, M., 2009. Sensitivity of *Tradescantia pallida* (Rose) Hunt. 'Purpurea'Boom to genotoxicity induced by ozone. Mutat. Res. - Genet. Toxicol. Environ. Mutagen. 675 (1–2), 41–45. https://doi.org/10.1016/j.mrgentox.2009.02.007.

Dumont, J., Keski-Saari, S., Keinänen, M., Cohen, D., Ningre, N., Kontunen-Soppela, S., Baldet, P., Gibon, Y., Dizengremel, P., Vaultier, M.N., Jolivet, Y., Oksanen, E., Le Thiec, D., 2014. Ozone affects ascorbate and glutathione biosynthesis as well as amino acid contents in three Euramerican poplar genotypes. Tree Physiol 34 (3), 253–266. https://doi.org/10.1093/treephys/tpu004.

Grulke, N.E., Heath, R.L., 2020. Ozone effects on plants in natural ecosystems. Plant Biol 22 (S1), 12–37. https://doi.org/10.1111/plb.12971.

Hoshika, Y., Pecori, F., Conese, I., Bardelli, T., Marchi, E., Manning, W.J., Badea, O., Paoletti, E., 2013. Effects of a three-year exposure to ambient ozone on biomass allocation in poplar using ethylenediurea. Environ. Pollut. 180, 299–303.

Hoshika, Y., Moura, B., Paoletti, E., 2018. Ozone risk assessment in three oak species as affected by soil water availability. Environ. Sci. Pollut. Res. 25, 8125–8136. https://doi.org/10.1007/s11356-017-9786-7.

Hoshika, Y., Carrari, E., Mariotti, B., Martini, S., De Marco, A., Sicard, P., Paoletti, E., 2020a. Flux-based ozone risk assessment for a plant injury index (pii) in three european cool-temperate deciduous tree species. Forests 11, 82. https://doi.org/10.3390/f11010082.

Hoshika, Y., Fares, S., Pellegrini, E., Conte, A., Paoletti, E., 2020b. Water use strategy affects avoidance of ozone stress by stomatal closure in Mediterranean trees - A modelling analysis. Plant Cell Environ 43, 611–623. https://doi.org/10.1111/pce.13700.

Hoshika, Y., Paoletti, E., Agathokleous, E., Sugai, T., Koike, T., 2020c. Developing ozone risk assessment for larch species. Front. For. Glob. Change 3, 45. https://doi.org/10.3389/ffgc.2020.00045.

Hoshika, Y., Paoletti, E., Centritto, M., Gomes, M.T.G., Puértolas, J., Haworth, M., 2022. Species-specific variation of photosynthesis and mesophyll conductance to ozone and drought in three Mediterranean oaks. Physiol. Plant. 174 (1), e13639. https://doi.org/10.1111/ppl.13639.

Innes, J.L., Skelly, J.M., Schaub, M., 2001. Ozone and Broadleaved Species. A Guide to the Identification of Ozone-induced Foliar Injury. Paul Haupt Verlag, Bern, p. 136.

Karnosky, D.F., Gielen, B., Ceulemans, R., Schlesinger, W.H., Norby, R.J., Oksanen, E., Matyssek, R., Hendrey, G.R., 2001. FACE systems for studying the impacts of greenhouse gases on forest ecosystems, in: The impact of carbon dioxide and other greenhouse gases on forest ecosystems. Report No. 3 of the IUFRO task force on environmental change. Wallingford UK CABI Publishing, pp. 297–324. https://doi.org/10.1079/9780851995519.0297.

Kuzminsky, E., Meschini, R., Terzoli, S., Pavani, L., Silvestri, C., Choury, Z., Scarascia-Mugnozza, G., 2016. Isolation of mesophyll protoplasts from mediterranean woody plants for the study of DNA integrity under abiotic stress. Front. Plant Sci. 7, 1168. https://doi.org/10.3389/fpls.2016.01168.

Langie, S.A., Azqueta, A., Collins, A.R., 2015. The comet assay: past, present, and future. Front. Genet. 6, 266. https://doi.org/10.3389/fgene.2015.00266.

Long, S.P., Bernacchi, C.J., 2003. Gas exchange measurements, what can they tell us about the underlying limitations to photosynthesis? procedures and sources of error. J. Exp. Bot. 54, 2393–2401. https://doi.org/10.1093/jxb/erg262.

Marchica, A., Lorenzini, G., Papini, R., Bernardi, R., Nali, C., Pellegrini, E., 2019. Signalling molecules responsive to ozone-induced oxidative stress in *Salvia officinalis*. Sci. Total Environ. 657, 568–576. https://doi.org/10.1016/j.scitotenv.2018.11.472.

Marzuoli, R., Gerosa, G., Desotgiu, R., Bussotti, F., Ballarin-Denti, A., 2009. Ozone fluxes and foliar injury development in the ozone-sensitive poplar clone oxford (*populus maximowiczii* × *populus berolinensis*): a dose-response analysis. Tree Physiol. 29, 67–76. https://doi.org/10.1093/treephys/tpn012.

Mills, G., Pleijel, H., Malley, C.S., Sinha, B., Cooper, O., Schultz, M., Neufeld, H.S., Simpson, D., Sharps, K., Feng, Z., Gerosa, G., Harmens, H., Kobayashi, K., Saxena, P., Paoletti, E., Sinha, V., Xu, X., 2018. Tropospheric ozone assessment report: present day tropospheric ozone distribution and trends relevant to vegetation. Elem. Sci. Anth 6, 47. https://doi.org/10.1525/elementa.302.

Meschini, R., Morucci, E., Berni, A., Lopez-Martinez, W., Palitti, F., 2015. Role of chromatin structure modulation by the histone deacetylase inhibitor trichostatin A on the radio-sensitivity of ataxia telangiectasia. Mutat. Res. - Fund. Mol. M 777, 52–59. https://doi.org/10.1016/j.mrfmmm.2015.04.009.

Moura, B.B., Brunetti, C., Engela, M., Hoshika, Y., Paoletti, E., Ferrini, F., 2021. Experimental assessment of ozone risk on ecotypes of the tropical tree *Moringa oleifera*. Environ. Res. 201, 111475 https://doi.org/10.1016/j.envres.2021.111475.

Moura, B.B., Paoletti, E., Badea, O., Ferrini, F., Hoshika, Y., 2022a. Visible foliar injury and ecophysiological responses to ozone and drought in oak seedlings. Plants 11 (14), 1836. https://doi.org/10.3390/plants11141836.

Moura, B.B., Carrari, E., Dalstein-Richier, L., Sicard, P., Leca, S., Badea, O., Pitar-Silaghi, D., Shashikumar, A., Ciriani, M., Paoletti, E., Hoshika, Y., 2022b. Bridging experimental and monitoring research for visible foliar injury as bio-indicator of ozone impacts on forests. Ecosyst. Health Sust. 8, 1. https://doi.org/10.1080/20964129.2022.2144466.

Nali, C., Paoletti, E., Marabottini, R., Della Rocca, G., Lorenzini, G., Paolacci, A.R., Ciaffi, M., Badiani, M., 2004. Ecophysiological and biochemical strategies of response to ozone in Mediterranean evergreen broadleaf species. Atmos. Environ. 38, 2247–2257. https://doi.org/10.1016/j.atmosenv.2003.11.043.

Paoletti, E., 2006. Impact of ozone on mediterranean forests: a review. Environ. Pollut. 144 (2), 463–474. https://doi.org/10.1016/j.envpol.2005.12.051.

Paoletti, E., 2007. Ozone Impacts On Forests, 2. CAB Rev.: Perspect, p. 13. https://doi.org/10.1079/PAVSNNR20072068.

Paoletti, E., Manning, W.J., 2007. Toward a biologically significant and usable standard for ozone that will also protect plants. Environ. Pollut. 150 (1), 85–95. https://doi.org/10.1016/j.envpol.2007.06.037.

Paoletti, E., Materassi, A., Fasano, G., Hoshika, Y., Carriero, G., Silaghi, D., Badea, O., 2017. A new-generation 3D ozone face (free air controlled exposure). Sci. Total Environ. 575, 1407–1414. https://doi.org/10.1016/j.scitotenv.2016.09.217.

Paoletti, E., Alivernini, A., Anav, A., Badea, O., Carrari, E., Chivulescu, S., Conte, A., Ciriani, M.L., Dalstein-Richier, L., De Marco, A., Fares, S., Fasano, G., Giovannelli, A., Lazzara, M., Leca, S., Materassi, A., Moretti, V., Pitar, D., Popa, I., Sabatini, F., Salvati, L., Sicard, P., Sorgi, T., Hoshika, Y., 2019. Toward stomatal–flux based forest protection against ozone: the MOTTLES approach. Sci. Total Environ. 691, 516–527. https://doi.org/10.1016/j.scitotenv.2019.06.525.

Paoletti, E., Sicard, P., Hoshika, Y., Fares, S., Badea, O., Pitar, D., Popa, I., Anav, A., Moura, B.B., De Marco, A., 2022. Towards long-term sustainability of stomatal ozone

flux monitoring at forest sites. Sustainable Horizons 2, 100018. https://doi.org/10.1016/j.horiz.2022.100018.

Piraino, F., Aina, R., Palin, L., Prato, N., Sgorbati, S., Santagostino, A., Citterio, S., 2006. Air quality biomonitoring: assessment of air pollution genotoxicity in the Province of Novara (North Italy) by using *Trifolium repens* L. and molecular markers. Sci. Total Environ. 372 (1), 350–359. https://doi.org/10.1016/j.scitotenv.2006.09.009.

Podda, A., Pisuttu, C., Hoshika, Y., Pellegrini, E., Carrari, E., Lorenzini, G., Nali, C., Cotrozzi, L., Zhang, L., Baraldi, R., Neri, L., Paoletti, E., 2019. Can nutrient fertilization mitigate the effects of ozone exposure on an ozone-sensitive poplar clone? Sci. Total Environ. 657, 340–350. https://doi.org/10.1016/j.scitotenv.2018.11.459.

Restivo, F.M., Laccone, M.C., Buschini, A., Rossi, C., Poli, P., 2002. Indoor and outdoor genotoxic load detected by the comet assay in leaves of *nicotiana tabacum* cultivars bel b and bel w3. Mutagenesis 17 (2), 127–134. https://doi.org/10.1093/mutage/17.2.127.

Rodrigues, G.S., Madkour, S.A., Weinstein, L.H., 1996. Genotoxic activity of ozone in *Tradescantia*. Environ. Exp. Bot. 36 (1), 45–50. https://doi.org/10.1016/0098-8472(95)00042-9.

Sacchelli, S., Carrari, E., Paoletti, E., Anav, A., Hoshika, Y., Sicard, P., Screpanti, A., Chirici, G., Cocozza, C., De Marco, A., 2021. Economic impacts of ambient ozone pollution on wood production in Italy. Sci. Rep. 11 (1), 1–9. https://doi.org/10.1038/s41598-020-80516-6.

Schaub, M., Calatayud, V., Ferretti, M., Brunialti, G., Lövblad, G., Krause, G.S.M., Sanz, M.J., 2016. Part VIII: monitoring of Ozone Injury. Manual On Methods and Criteria for Harmonized Sampling, Assessment, Monitoring and Analysis of the Effects of Air Pollution On Forests; UNECE ICP Forests Programme Coordinating Centre, ed. UNECE ICP Forests Programme Coordinating Centre, 14. Eberswalde. Germany: Thünen Institute of Forest Ecosystems.

Sicard, P., Anav, A., De Marco, A., Paoletti, E., 2017. Projected global tropospheric ozone impacts on vegetation under different emission and climate scenarios. Atmos. Chem. Phys. 17 (19), 12177–12196. https://doi.org/10.5194/acp-17-12177-2017.

Singh, A.A., 2022. Biomonitoring potential of tropospheric ozone in plants utilizing visible injury and biomarkers. New Paradigms in Environmental Biomonitoring Using Plants. Elsevier, pp. 181–224. https://doi.org/10.1016/B978-0-12-824351-0.00008-0.

Tai, H.H., Percy, K.E., Karnosky, D.F., 2010. DNA damage in *populus tremuloides* clones exposed to elevated O3. Environ. Pollut. 158 (4), 969–976. https://doi.org/10.1016/j.envpol.2009.10.005.

Tseng, Y.T., Lin, K.C., 2015. Effects of volatile organic compound ether on cell responses and gene expressions in arabidopsis. Bot. Stud. 57 (1), 1–9. https://doi.org/10.1186/s40529-015-0112-8.

Turcsanyi, E., Lyons, T., Plochl, M., Barnes, J., 2000. Does ascorbate in the mesophyll cell walls form the first line of defence against ozone? Testing the concept using broad bean (*Vicia faba* L.). J. Exp. Bot. 51 (346), 901–910. https://doi.org/10.1093/jexbot/51.346.901.

Tuteja, N., Singh, M.B., Misra, M.K., Bhalla, P.L., Tuteja, R., 2001. Molecular mechanisms of DNA damage and repair: progress in plants. Crit. Rev. Biochem. Mol. Biol. 36 (4), 337–397. https://doi.org/10.1080/20014091074219.

Vainonen, J.P., Kangasjärvi, J., 2015. Plant signalling in acute ozone exposure. Plant Cell Environ 38, 240–252. https://doi.org/10.1111/pce.12273.

Victorin, K., 1992. Review of the genotoxicity of ozone. Mutat. Res. - Genet. Toxicol. 277 (3), 221–238. https://doi.org/10.1016/0165-1110(92)90045-b.

Watanabe, M., Hoshika, Y., Koike, T., 2014. Photosynthetic responses of Monarch birch seedlings to differing timings of free air ozone fumigation. J. Plant Res. 127, 339–345. https://doi.org/10.1007/s10265-013-0622-y.

World Health Organization (WHO), 2021. Global Air Quality Guidelines: Particulate Matter (PM2.5 and PM10), Ozone, Nitrogen Dioxide, Sulfur Dioxide and Carbon Monoxide: Executive Summary. World Health Organization, Geneva.

Yoshiyama, K.O., Sakaguchi, K., Kimura, S., 2013. DNA damage response in plants: conserved and variable response compared to animals. Biology 2 (4), 1338–1356. https://doi.org/10.3390/biology2041338.

Young, P.J., Archibald, A.T., Bowman, K.W., Lamarque, J.F., Naik, V., Stevenson, D.S., Tilmes, S., Voulgarakis, A., Wild, O., Bergmann, D., Cameron-Smith, P., Cionni, I., Collins, W.J., Dalsøren, S.B., Doherty, R.M., Eyring, V., Faluvegi, G., Horowitz, L.W., Josse, B., Lee, Y.H., MacKenzie, I.A., Nagashima, T., Plummer, D.A., Righi, M., Rumbold, S.T., Skeie, R.B., Shindell, D.T., Strode, S.A., Sudo, K., Szopa, S., Zeng, G., 2013. Pre-industrial to end 21st century projections of tropospheric ozone from the atmospheric chemistry and climate model intercomparison project (ACCMIP). Atmos. Chem. Phys. 13, 2063–2090. https://doi.org/10.5194/acp-13-2063-2013.

Zhang, L., Hoshika, Y., Carrari, E., Burkey, K., Paoletti, E., 2018. Protecting the photosynthetic performance of snap bean under free-air ozone exposure. J. Environ. Sci. 66, 31–40. https://doi.org/10.1016/j.jes.2017.05.009.